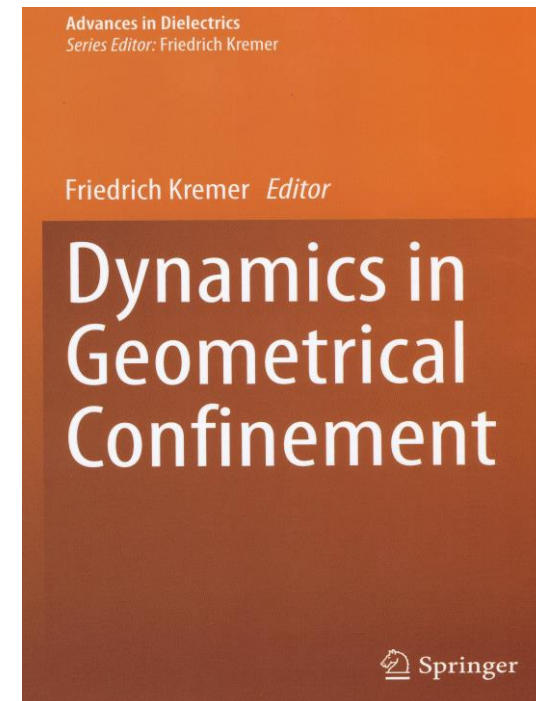


**UNIVERSITY OF LEIPZIG**

**Faculty of Physics and Earth Sciences  
Department of Experimental Physics I**

**Group “Molecule physics”**



**Annual Report 2014**

**Cover picture:**

“Dynamics in Geometrical Confinement” is the second volume in the series Advances in Dielectrics (Ed. F. Kremer).

Low molecular weight and polymeric molecules can be constrained under conditions of geometrical confinement having different dimensionalities:

- (i) in nanometer thin layers or self-supporting films (one-dimensional),
- (ii) in pores or tubes having nanometric diameter (two-dimensional) or
- (iii) as micelles embedded in some matrix (three-dimensional) or as nanodroplets.

Within the last two decades, their dynamics under such conditions has been the focus of intense worldwide research activities. Evidence exists that the overall molecular mobility results from a subtle balance between surface and confinement effects. Due to attractive guest/host interactions, the former causes a slowing down of the molecular dynamics, which can be compensated by an appropriate surface coating. The latter is characterized by an increase in the mobility, which becomes more pronounced with decreasing external length scale, e.g., film thickness or pore diameter. In this case, modification of the host/guest interaction by surface treatment has negligible or no effect. Broadband Dielectric Spectroscopy (BDS) plays an essential role in these studies. It is the intention of this second volume in the series “Advances in Dielectrics” to summarize the state of the art in this emerging field, which is also of fundamental importance for nanotechnology.

**UNIVERSITÄT LEIPZIG**

Fakultät für Physik und Geowissenschaften  
Prof. Dr. Friedrich Kremer  
Linnéstraße 5  
04103 Leipzig  
Germany

Tel.: (0341) 97-32550  
Fax: (0341) 97-32599  
e-mail: [kremer@physik.uni-leipzig.de](mailto:kremer@physik.uni-leipzig.de)

### **The year 2014**

This is my last report as an active professor; in March 2015 I shall retire. But this does not mean that I intend to move away from research. Instead, I plan to focus on the fields of Broadband Dielectric and Fourier Transform Infrared Spectroscopy; in both we have profound expertise and the two have proven to be complementary and highly versatile in the physics of soft and hard condensed matter. In detail it is planned to study the dielectric properties of polymeric Ionic Liquids (PIL), a project already being funded by the German Science Foundation within a "Knowledge-transfer-project (Erkenntnis-transferprojekt)" together with Prof. Veronika Strehmel, FH Krefeld and Merck KGaA in Darmstadt. Currently under review for the second funding period (2015 - 2019) is an application - titled "Broadband Dielectric and IR Spectroscopy to study molecular dynamics and order in nanometer domains of end-fixed polymers" - within the Collaborative Research Center (CRC) of the universities in Halle and Leipzig, "Polymers under multiple constraints: restricted and controlled molecular order and mobility". Furthermore a common endeavor together with researchers from veterinary medicine is under discussion and might soon become concretized. In summary, I plan to have a research team of about 4 PhD students and one Postdoc. Additionally, several book projects are envisaged within the series "Advances in Dielectrics". So I look forward to pursue research in soft matter physics with utmost engagement and ambition.

January 2015

Friedrich Kremer

## Contents

	page
Preface	1
1. Organization of the group	3
2. Projects	4
2.1 Data analysis for nano-structured electrode arrangements M. Tress, N. Neubauer, R. Winkler, P. Uhlmann, E.U. Mapesa, M. Reiche, and <u>F. Kremer</u>	4
2.2 Dielectric properties of high permittivity siloxanes S.J. Düнки, M. Tress, <u>F. Kremer</u> , S. Ko, F.A. Nüesch, C. Racles, and <u>D.M. Opris</u>	5
2.3 Molecular dynamics of itraconazole confined in thin supported layers <u>E.U. Mapesa</u> , M. Tarnacka, M. Tress, W. K. Kipnusu, K. Kamiński and F. Kremer	6
2.4 Structure and Dynamics of Asymmetric Poly(styrene- <i>b</i> -1,4-isoprene) Diblock Copolymer under 1D and 2D Nanoconfinement W.K. Kipnusu, M.M. Elmahdy, E.U. Mapesa, J. Zhang, W. Böhlmann, D-M. Smilgies, C.M. Papadakis and <u>F. Kremer</u>	7
2.5 Hydrogen-bonded chain length equilibria in mono-hydroxyl alcohol under nano-confinement W.K.Kipnusu, K. Kaminiski, and <u>F. Kremer</u>	8
2.6 Inter- and intra-molecular dynamics in polyalcohols during glass transition L. Popp, W. Kossack, M. Treß, W.K. Kipnusu and <u>F. Kremer</u>	9
2.7 Strain induced, anisotropic crystallization studied by FTIR <u>W. Kossack</u> , A. Seidlitz*, T. Thurn-Albrecht*, <u>F. Kremer</u>	10
2.8 Relaxations and charge transport in Polymeric Ionic Liquids F. Frenzel, M.Y. Folikumah, M. Schulz, W.H. Binder, and <u>F. Kremer</u>	11
2.9 Glassy dynamics of Poly(2-Vinyl-Pyridine) brushes with varying grafting density N. Neubauer, R. Winkler, M. Treß, P. Uhlmann, M. Reiche, and <u>F. Kremer</u>	12
2.10 Methods to determine the pressure dependence of the molecular order parameter in (bio)macromolecular fibers A. M. Anton, C. Gutsche, W. Kossack, and <u>F. Kremer</u>	13
2.11 IR transition moment orientational analysis (IR-TMOA) on the surface-induced orientation in thin layers of a high electron mobility n-type copolymer (P[NDI2OD-T2]) <u>A. M. Anton</u> , R. Steyrlleuthner, W. Kossack, D. Neher, and <u>F. Kremer</u>	14
2.12 The influence of shear processing on the morphology orientation and mechanical properties of styrene butadiene triblock copolymers N. Mahmood, A. M. Anton, G. Gupta, Tm Bambur, K. Knoll, T. Thurn-Albrecht, <u>F. Kremer</u> , <u>M. Beiner</u>	15
2.13 Epitope-Scans of monoclonal antibody HPT-101 using dynamic force spectroscopy sand ELISA T. Stangner, S. Angioletti-Uberti, D. Knappe, D. Singer, C. Wagner, C. Gutsche, J. Dzubiella, R. Hoffmann, <u>F. Kremer</u>	16
3. Publications	17
4. Financial Support	18
5. Graduations	19
6. Industry collaborations	19

## 5. Graduations

### Habilitation :

Dr. Periklis Papadopoulos  
"Active swimmers" - selbstgetriebene Bewegung von Kolloiden"

### Doctoral degree:

DP Emmanuel Urandu Mapesa  
"Molecular dynamics of nanometric layers of glass formers in interaction with solid substrates"

DP Martin Treß  
"Breitbandige dielektrische Spektroskopie zur Untersuchung der molekularen Dynamik von Nanometer-dünnen Polymerschichten"

### Bachelor of Science:

Benjamin Suttner  
"Intramolekulare Dynamik von niedermolekularen organischen Glasbildnern"

## 6. Industry collaborations

### Novocontrol

Hundsangen, Germany

### BOREALIS Polyolefine GmbH

Linz, Austria

### Süd-Chemie AG

München, Germany

### MERCK KGaA

Darmstadt, Germany

## 4. Financial support

### Prof. Dr. F. Kremer

**FOR 877** "From local constraints to macroscopic transport" TP 7 "Electric field driven motion of single polyelectrolyte grafted colloids"  
KR 1138/21-2 (2011-2014)

### Prof. Dr. F. Kremer

**SPP 1369** "Polymer-Solid Contacts: Interfaces and Interphases"  
TP "Interfacial dynamics of polymers in interaction with solid substrates"  
KR 1138/23-2 (2011–2014)

### Prof. Dr. F. Kremer

Graduate School "Leipzig School of Natural Sciences –Building with Molecules and Nano-objects" **BuildMoNa**, TP 15 "Dynamics of DNA under tension and in confinement"  
GSC 185/1 (2008-2014)

**Prof. Dr. F. Kremer** was Principal Investigator in the "Leipzig School of Natural Sciences – Building with Molecules and Nano-Objects" in the framework of a Graduate School funded by the "**Federal Excellence Initiative**". This supported several Ph.D. projects.

### Prof. Dr. F. Kremer

**SFB/TRR 102** "Polymers under multiple constraints: restricted and controlled molecular order and mobility"  
TP **B05** "Structural levels of organisation in spider-silk - a combined mechanical and IR-spectroscopic study" (2011-2015)  
TP **B08** "Broadband Dielectric Spectroscopy to study the molecular dynamics in nanometer thin layers of block copolymers" (2011-2015)

**Prof. Dr. F. Kremer** is deputy chairman of the **SFB-TRR 102** on "**Polymers under multiple constraints: restricted and controlled molecular order and mobility**" of the Universities of Halle and Leipzig.

**Prof. Dr. F. Kremer** (Prof. Dr. Veronika Strehmel, Hochschule Niederrhein)

**New Polymer Materials on the Basis of Functionalized Ionic Liquids for Application in Membranes** "Knowledge Transfer Project"  
KR 1138/24-1; STR 437/5-3; (2014- 2017)

## 1. Organization of the group

**Head:** Prof. Dr. Friedrich Kremer

### Academic Staff and Postdocs

Dr. Mahdy M. Elmahdy

### Doctorands and Students

Dipl.-Phys. Markus Anton  
M. Sc. Wycliffe Kiprof Kipnusu  
Dipl.-Phys. Wilhelm Kossack  
Dipl.-Phys. Nils Neubauer  
M. Sc. Emmanuel Urandu Mapesa  
Dipl.-Phys. Tim Stangner  
Dipl.-Phys. Martin Treß

cand. B. Sc. Falk Frenzel  
cand. M.Sc. Ludwig Popp  
cand. M. Sc. Benjamin Suttner

### Technical staff

Dipl.-Phys. Cordula Bärbel Krause  
Kerstin Lohse  
Dipl.-Ing. (FH) Jörg Reinmuth  
Dipl.-Phys. Wiktor Skokow

### Guests

Dr. Jun Ma

### Alumni

Prof. Dr. Siegbert Grande

## 2. Projects

### 2.1 Data analysis for nano-structured electrode arrangements

M. Tress, N. Neubauer, R. Winkler, P. Uhlmann, E. U. Mapesa, M. Reiche and F. Kremer

The development of nano-structured electrodes [1] moved Broadband Dielectric Spectroscopy into the field of interfacial techniques [2] and recent refinements succeeded to employ this method to block copolymers [3], polymer brushes [4] and even isolated polymer chains [5]. Such systems cannot be studied with conventional methods since only the free surface i) enables mesoscopic structural rearrangements (block copolymers, brushes) and ii) avoids electrical short cuts in un-continuously covered samples (isolated chains). On the other hand, as a result the probe volume contains several different materials which contribute in a non-trivial way to the total response.

To unwrap the latter and extract the net dielectric properties of the sample material, a sophisticated fit function is employed. For that, an equivalent circuit describing the spatial distribution of all components is created [6]. Exemplarily, Fig. 1 displays the cross section of poly(2-vinylpyridine) (P2VP) brushes grafted to a poly(glycidyl methacrylate) (PGMA) anchoring layer and the respective equivalent circuit. Consequently, the fit function derived from the latter does not only contain parameters for the dielectric properties of all components but also implements their geometrical distribution. This enables a quantitative

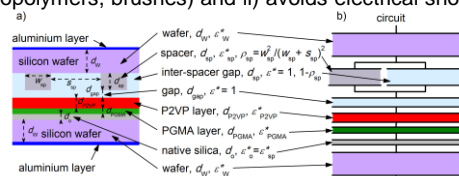


Fig. 1: a) Schematic cross-section of P2VP brushes in the nano-structured electrode arrangement anchored on a PGMA layer. b) Equivalent circuit.

description of the data which can explain features like the polarization process induced by the conductivity of P2VP (Fig. 2).

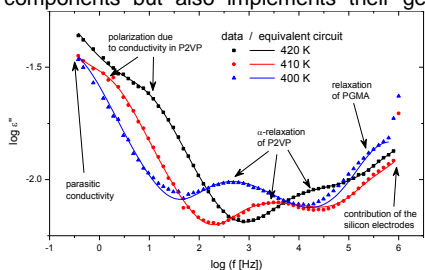


Fig. 2: Dielectric loss spectra of 6.4-nm-thick P2VP polymer brushes grafted to a PGMA anchoring layer (2.5 nm) in the nano-structured electrode arrangement (temperatures as indicated). Solid lines represent fits with the equivalent circuit model which contains the geometrical measures of the sample.

#### References:

- [1] A. Serghei and F. Kremer, *Rev Sci Inst* **79** 026101 (2008)
- [2] A. Serghei, H. Huth, C. Schick and F. Kremer, *Macromol* **41** 3636 (2008); M. Erber, M. Tress, E.U. Mapesa, A. Serghei, K.-J. Eichhorn, B. Voit and F. Kremer, *Macromol* **43** 7729 (2010); M. Tress, M. Erber, E.U. Mapesa, H. Huth, J. Müller, A. Serghei, C. Schick, K.-J. Eichhorn, B. Voit and F. Kremer, *Macromol* **43** 9937 (2010); E.U. Mapesa, M. Erber, M. Tress, K.J. Eichhorn, A. Serghei, B. Voit and F. Kremer, *Eur Phys J: Spec Top* **189** 173 (2010); E.U. Mapesa, M. Tress, G. Schulz, H. Huth, C. Schick, M. Reiche, and F. Kremer, *Soft Matter* **9** 10592 (2013); E.U. Mapesa, L. Popp, W.K. Kipnusu, M. Tress, and F. Kremer, *Soft Materials* **12** S22 (2014); E.U. Mapesa, M. Tarnacka, E. Kaminska, K. Adrjanowicz, M. Dulski, M. Tress, W. Kossack, W.K. Kipnusu, K. Kaminski, and F. Kremer, *RSC Adv.* **4** 28432 (2014)
- [3] W.K. Kipnusu, M.M. Elmahdy, M. Tress, M. Fuchs, E.U. Mapesa, D.-M. Smilgies, J. Zhang, C.M. Papadakis, and F. Kremer, *Macromol* **46** 9729 (2013)
- [4] N. Neubauer, R. Winkler, M. Tress, P. Uhlmann, M. Reiche, and F. Kremer, (submitted)
- [5] M. Tress, E.U. Mapesa, W. Kossack, W.K. Kipnusu, M. Reiche and F. Kremer, *Science* **341** 1371 (2013)
- [6] M. Tress, E.U. Mapesa, W. Kossack, W.K. Kipnusu, M. Reiche, and F. Kremer in Kremer, F. (Ed.) *Dynamics in Geometrical Confinement*, Springer International Publishing, **2014**, 61-93

**Collaborations:** (1) Max-Planck-Institute for Microstructures, Halle, and (2) MicroFAB Bremen

**Funding:** BuildMoNa, DFG priority program SPP1369 and SFB TRR 102

## 3. Publications

1. Griffin, P.J., A.P. Holt, Y. Wang, V.N. Novikov, J.R. Sangoro, F. Kremer, A.P. Sokolov "Interplay Between Hydrophobic Aggregation and Charge Transport in the Ionic Liquid Methyltrioctylammonium Bis(trifluoromethylsulfonyl)imide" *J. Phys. Chem. B* **118**, 783-790 (2014) DOI: 10.1021/jp412365n
2. Sangoro, J.R., C. Iacob, A.L. Agapov, Y. Wang, S. Berdzinski, H. Rexhausen, V. Strehmel, C. Friedrich, A.P. Sokolov, F. Kremer "Decoupling of ionic conductivity from structural dynamics in polymerized ionic liquids" *Soft Matter* **10**, (20) 3536-402014 (2014) DOI: 10.1039/c3sm53202j
3. Kossack, W., W.K. Kipnusu, M. Dulski, K. Adrjanowicz, O., E. Kaminska, E.U. Mapesa, M. Tress, K. Kaminski, F. Kremer "The kinetics of mutarotation in L-fucose as monitored by dielectric and infrared spectroscopy" *J. Chem. Phys.* **140**, 215101 (2014) DOI: 10.1063/1.4880718
4. Mapesa, E.U., L. Popp, W.K. Kipnusu, M. Tress, F. Kremer "Molecular dynamics in 1- and 2-D confinement as studied for the case of poly(cis-1,4-isoprene)" *Soft Materials* **12**, 22-30 DOI: 10.1080/1539445X.2014.928320
5. Mahmood, N., A.M. Anton, G. Gupta, T. Babur, K. Knoll, T. Thurn-Albrecht, F. Kremer, M. Beiner, R. Weidisch "Influence of shear processing on morphology orientation and mechanical properties of styrene butadiene triblock copolymers" *Polymer* **55**, 3782-3791 (2014) DOI: 10.1016/j.polymer.2014.05.062
6. Tress, M., E.U. Mapesa, W. Kossack, W.K. Kipnusu, M. Reiche, F. Kremer "Molecular dynamics of condensed (semi-) isolated polymer chains" in: "Dynamics in Geometrical Confinement", F. Kremer (Ed.) Springer-Verlag (2014) ISBN 978-3-319-06099-6
7. Mapesa, E.U., M. Tress, M. Reiche, F. Kremer "Molecular dynamics of poly(cis-1,4-isoprene) in 1- and 2-dimensional confinement" in: "Dynamics in Geometrical Confinement", F. Kremer (Ed.) Springer-Verlag (2014) ISBN 978-3-319-06099-6
8. Kipnusu, W.K., C. Iacob, M. Jasiurkowska-Delaporte, W. Kossack, J.R. Sangoro, F. Kremer "Rotational diffusion of guest molecules confined in uni-directional nanopores" in: "Dynamics in Geometrical Confinement", F. Kremer (Ed.) Springer-Verlag (2014) ISBN 978-3-319-06099-6
9. Iacob, C., J.R. Sangoro, W.K. Kipnusu, F. Kremer "Rotational and Translation Diffusion of Ionic Liquids in Silica Nanopores" in: "Dynamics in Geometrical Confinement", F. Kremer (Ed.) Springer-Verlag (2014) ISBN 978-3-319-06099-6
10. Mapesa, E.U., M. Tarnacka, E. Kaminska, K. Adrjanowicz, M. Dulski, W. Kossack, M. Tress, W.K. Kipnusu, K. Kaminski, F. Kremer "Molecular dynamics of itraconazole confined in thin supported layers" *RSC Adv.* **4**, 28432 (2014) DOI: 10.1039/c4ra01544d
11. Kipnusu W.K., P. Zeigermann, C. Iacob, F. Kremer, M. Schoen, M.G. Mazza, R. Valiullin "Experimental evidence of enhanced transport in supernematics" *Soft Condensed Matter* (2014) arXiv: 1406.5868

## 2.13 Epitope-Scans of monoclonal antibody HPT-101 using dynamic force spectroscopy and ELISA

T. Stangner, S. Angioletti-Uberti, D. Knappe, D. Singer, C. Wagner, C. Gutsche, J. Dzubiella, R. Hoffmann, F. Kremer

Monoclonal antibodies (mAbs) are nowadays widely used as medical agents in therapy and diagnostics. Especially in the context of neurodegenerative diseases (e.g. Alzheimer's disease), when symptoms are heterogeneous or their initial manifestation is ambiguous and can be mistaken with that of other conditions, the specificity of mAbs is a key feature for the early stage diagnosis of the disease [1]. Therefore, we analyze binding of the phosphorylation-specific monoclonal antibody HPT-101 to the peptide tau[pThr231/pSer235] carrying two potential phosphorylation sites (Thr231 and Ser235), being the most probable markers for Alzheimer's disease. In order to determine the antibody epitope, seven tau-isoforms were synthesized from the parent peptide by replacing binding relevant amino acids with a neutral alanine (alanine-scan). The interactions between the modified peptides and mAb HPT-101 were investigated using ELISA and optical tweezers-assisted dynamic force spectroscopy. The latter allows characterizing the binding between the peptide and antibody on a single-molecule level [2,3]. By comparing the results from both methods, we were able to categorize the importance of each amino acid. Thereby, we found four essential, two beneficial (secondary) and one non-essential amino acid for the interaction between the mAb and the parent peptide. In conclusion, we were able to identify the target epitope of the monoclonal antibody HPT-101 by means of single amino acids.

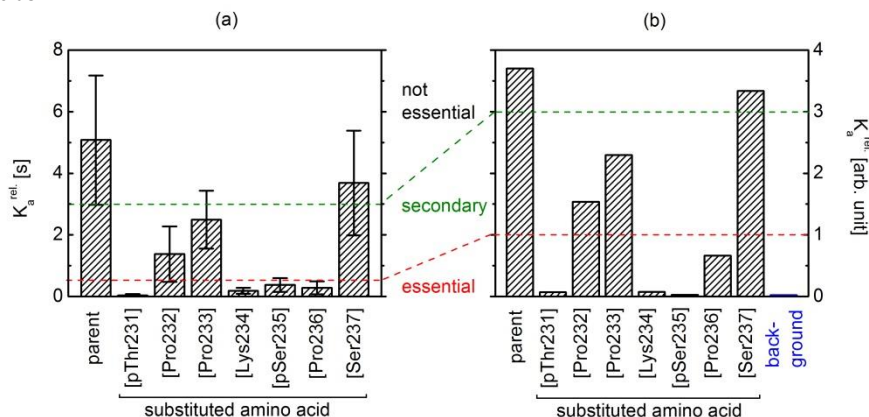


**Fig. 1:** Comparison of the affinity constant  $K_a^{\text{rel}}$  of mAb HPT-101 to the parent peptide and its isoforms using dynamic force spectroscopy (a) and ELISA (b) measurements. In agreement of both approaches, four essential, two secondary and one non-essential amino acid can be determined for the interaction between mAb HPT-101 and the parent peptide tau[pThr231/pSer235].

### References:

- [1] D.J. Cahill, *Journal of Immunological Methodes*, 2001, 250, 81–91.
- [1] Wagner et al., *Soft Matter*, 2011, 7, 4370-4378
- [2] Stangner et al., *ACS Nano* 2013, 7, 12, 11388

**Collaborations:** Biotechnologisch-Biomedizinisches Zentrum Leipzig, TU Berlin

**Funding:** ESF, BuildMoNa

## 2.2 Dielectric properties of high permittivity siloxanes

S. J. Dünki<sup>1,2</sup>, M. Tress, F. Kremer, S. Y. Ko<sup>1,2</sup>, F. A. Nüesch<sup>1,2</sup>, C. Racles<sup>3</sup> and D. M. Opris<sup>1</sup>

A homologous series of novel siloxane polymers with fine-tuned glass transition temperatures and dielectric properties by utilizing thiol-ene post-polymerization reactions is presented [1]. The pendent vinyl groups of a high molecular weight polymethylvinylsiloxane were exhaustively reacted with the thiol compounds 1-butanethiol and 3-mercaptopropionitrile both separately to give polymers **P2** and **P3**, respectively, as well as in various ratios  $x, y$  so as to create materials **P2<sub>x</sub>P3<sub>y</sub>** with greatly differing contents of the polar nitrile group  $y$  (Fig. 1 scheme). Because of the presence of the polarizable thioether and nitrile groups, the resulting siloxane polymers exhibit permittivity ranging from  $\epsilon' = 4.7$  to 18.4 for **P2** and **P3**, respectively. Due to their high permittivity, these polymers are attractive candidates for dielectric elastomer actuators and flexible electronics.

The BDS measurements in a broad frequency and temperature range reveal the segmental

relaxation of the siloxane backbone (Fig. 1);

the scaling with  $T_g$  verifies that this is the structural relaxation underlying glassy dynamics.

Another process with non-Arrhenius type thermal activation is, according to other studies of PDMS, ascribed to the relaxation of segments neighbouring crystallites. Two secondary relaxations (Fig. 2), a fast and a slow one, can be assigned to local fluctuations of the two types of side chain end groups (methyl and nitrile groups, respectively). This is evident from the differences in the dynamics, in the activation energies and in the dielectric relaxation strength.

This is evident from the differences in the dynamics, in the activation energies and in the dielectric relaxation strength.

This is evident from the differences in the dynamics, in the activation energies and in the dielectric relaxation strength.

This is evident from the differences in the dynamics, in the activation energies and in the dielectric relaxation strength.

This is evident from the differences in the dynamics, in the activation energies and in the dielectric relaxation strength.

This is evident from the differences in the dynamics, in the activation energies and in the dielectric relaxation strength.

This is evident from the differences in the dynamics, in the activation energies and in the dielectric relaxation strength.

This is evident from the differences in the dynamics, in the activation energies and in the dielectric relaxation strength.

This is evident from the differences in the dynamics, in the activation energies and in the dielectric relaxation strength.

This is evident from the differences in the dynamics, in the activation energies and in the dielectric relaxation strength.

This is evident from the differences in the dynamics, in the activation energies and in the dielectric relaxation strength.

This is evident from the differences in the dynamics, in the activation energies and in the dielectric relaxation strength.

This is evident from the differences in the dynamics, in the activation energies and in the dielectric relaxation strength.

This is evident from the differences in the dynamics, in the activation energies and in the dielectric relaxation strength.

This is evident from the differences in the dynamics, in the activation energies and in the dielectric relaxation strength.

This is evident from the differences in the dynamics, in the activation energies and in the dielectric relaxation strength.

This is evident from the differences in the dynamics, in the activation energies and in the dielectric relaxation strength.

This is evident from the differences in the dynamics, in the activation energies and in the dielectric relaxation strength.

This is evident from the differences in the dynamics, in the activation energies and in the dielectric relaxation strength.

This is evident from the differences in the dynamics, in the activation energies and in the dielectric relaxation strength.

This is evident from the differences in the dynamics, in the activation energies and in the dielectric relaxation strength.

This is evident from the differences in the dynamics, in the activation energies and in the dielectric relaxation strength.

This is evident from the differences in the dynamics, in the activation energies and in the dielectric relaxation strength.

This is evident from the differences in the dynamics, in the activation energies and in the dielectric relaxation strength.

This is evident from the differences in the dynamics, in the activation energies and in the dielectric relaxation strength.

This is evident from the differences in the dynamics, in the activation energies and in the dielectric relaxation strength.

This is evident from the differences in the dynamics, in the activation energies and in the dielectric relaxation strength.

This is evident from the differences in the dynamics, in the activation energies and in the dielectric relaxation strength.

This is evident from the differences in the dynamics, in the activation energies and in the dielectric relaxation strength.

This is evident from the differences in the dynamics, in the activation energies and in the dielectric relaxation strength.

This is evident from the differences in the dynamics, in the activation energies and in the dielectric relaxation strength.

This is evident from the differences in the dynamics, in the activation energies and in the dielectric relaxation strength.

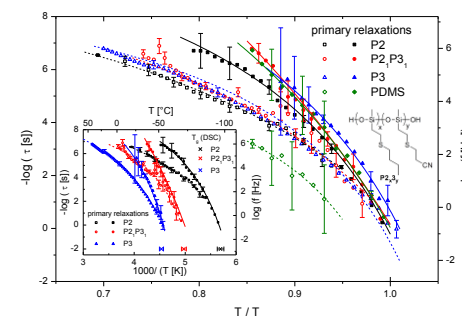


**Fig. 1:** Mean relaxation time  $\tau$  of the primary relaxations of the polymers **P2**, **P2,P3**, and **P3** as a function of absolute inverse temperature (inset) and rescaled with respect to the corresponding calorimetric glass transition temperature  $T_g$  (main frame). Solid and dashed lines are fits of the Vogel-Fulcher-Tammann equation to the data of the  $\alpha$ -relaxation in the amorphous phase (solid symbols) and the segments neighbouring the crystallites (open symbols), respectively. In the main frame, also the chemical structure of **P2<sub>x</sub>P3<sub>y</sub>** is depicted.

relaxation of the siloxane backbone (Fig. 1); the scaling with  $T_g$  verifies that this is the structural relaxation underlying glassy dynamics. Another process with non-Arrhenius type thermal activation is, according to other studies of PDMS, ascribed to the relaxation of segments neighbouring crystallites. Two secondary relaxations (Fig. 2), a fast and a slow one, can be assigned to local fluctuations of the two types of side chain end groups (methyl and nitrile groups, respectively). This is evident from the differences in the dynamics, in the activation energies and in the dielectric relaxation strength.

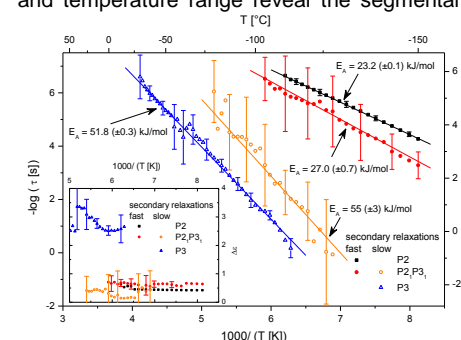


**Fig. 2:** Mean relaxation time  $\tau$  as a function of inverse temperature of the secondary relaxations of the polymers **P2**, **P2,P3**, and **P3**. Inset: Dielectric relaxation strength  $\Delta\epsilon$  of these relaxations as a function of inverse temperature.

**Collaborations:** (1) Empa, Swiss Federal Laboratories for Materials Science and Technology (2) Ecole Polytechnique Fédérale de Lausanne (3) Petru Poni Institute of Macromolecular Chemistry, Romania

### References:

- [1] S. J. Dünki, M. Tress, F. Kremer, S. Y. Ko, F. A. Nüesch, C. Racles and D. M. Opris, submitted (2014)

## 2.3 Molecular dynamics of itraconazole confined in thin supported layers

E.U. Mapesa, M. Tarnacka\*, M. Tress, W. K. Kipnusu, K. Kamiński\* and F. Kremer

For the first time, we studied a liquid crystalline material under one-dimensional nanoconfinement. Broadband Dielectric Spectroscopy (BDS) was used to study the molecular dynamics of thin layers of itraconazole – an active pharmaceutical ingredient with rod-like structure and whose Differential Scanning Calorimetry (DSC) scans reveal liquid crystalline-like phase transitions. It is found that (i) the structural relaxation process remains bulk like, within the limits of experimental accuracy, in its mean relaxation rate (Figure 1), while (ii) its shape is governed by two competing events (Figure 2): interfacial interactions, and crystalline ordering. Additionally, (iii) the dynamics of the  $\delta$ -relaxation – assigned to the flip-flop rotation of the molecule about its short axis – deviate from bulk behaviour as the glass transition is approached for the confined material. In a recently published paper [1], these observations are rationalized within the framework of molecular dynamics as currently understood.

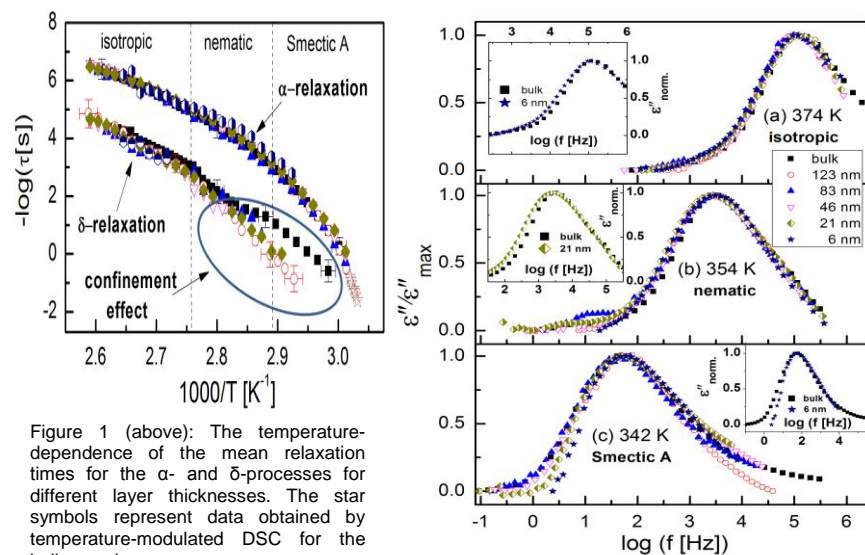


Figure 1 (above): The temperature-dependence of the mean relaxation times for the  $\alpha$ - and  $\delta$ -processes for different layer thicknesses. The star symbols represent data obtained by temperature-modulated DSC for the bulk sample.

Figure 2 (on the right): Dielectric spectra normalized with respect to the maximum of dielectric loss ( $\epsilon''_{\max}$ ) of the  $\alpha$ -process at temperatures where the (a) isotropic, (b) nematic and (c) smectic A mesophases are expected. The insets in (a) and (b) compare data for bulk sample and thin films (thicknesses as indicated) at 374 and 354 K, respectively.

### References

[1] E.U. Mapesa, M. Tarnacka, E. Kamińska, K. Adrjanowicz, M. Dulski, W. Kossack, M. Tress, W.K. Kipnusu, K. Kamiński, and F. Kremer, RSC Adv. 4, 28432 (2014)

### Funding:

Financial support from DFG (SPP 1369 and SFB TRR 102) is greatly acknowledged.

### Collaboration:

Max-Planck Institute for Microstructure Physics, Halle (Saale) \*Institute of Physics, University of Silesia, ul. Uniwersytecka 4, 40-007 Katowice, Poland

## 2.12 The influence of shear processing on the morphology orientation and mechanical properties of styrene butadiene triblock copolymers

N. Mahmood, A. M. Anton, G. Gupta, Tm Bambur, K. Knoll, T. Thurn-Albrecht, F. Kremer, M. Beiner, and R. Weidisch

The influence of ram extrusion on structure and mechanical properties of a triblock copolymer consisting of polystyrene (S) outer blocks and poly(styrene-stat-butadiene) (S/B) middle block is studied for a wide range of shear rates. Structural features on the mesoscale (10-100 nm) are investigated by small angle x-ray scattering (SAXS) and transmission electron microscopy (TEM). Transition Moment Orientational Analysis (TMOA) is applied to quantify the orientation on the molecular (segmental) scale ( $< 1$  nm). All extruded samples microphase-separate and show a lamellar morphology with periodicities of about 33 nm. Significant orientation is observed on the mesoscale where the surface normals of the lamellae are preferentially perpendicular to the extrusion direction. The corresponding degree of orientation drops slightly at elevated shear rates of about  $600 \text{ s}^{-1}$ . In contrast, significant orientation on the molecular scale is absent for styrene and butadiene units indicating basically random orientation of the chain segments. The mechanical properties are, however, strongly anisotropic. In general, the results demonstrate that orientation effects on the mesoscale have a strong influence on the mechanical properties and must be considered during the optimization of extruded or injection-molded components made from microphase-separated block polymers.

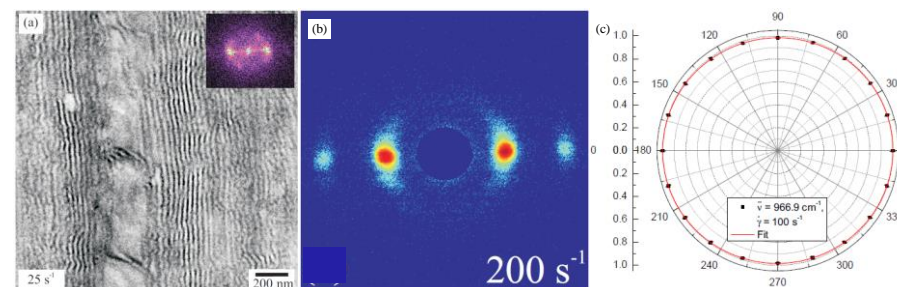


Fig. 1: TEM (a), SAXS (b), and IR-TMOA (c) measurement on S-S/B-S triblock copolymer. On the mesoscale well-defined and well-aligned lamella structures are evident (a and b). In contrast, the circular shape of the polarization-dependent oscillator strength indicates absence of any molecular orientation on the segmental scale (c).

### References:

[1] N. Mahmood, A. M. Anton, G. Gupta, Tm Bambur, K. Knoll, T. Thurn-Albrecht, F. Kremer, M. Beiner, R. Weidisch, Polymer (2014) 55, 3782-3791

**Collaborations:** (1) Martin-Luther-Universität Halle-Wittenberg, Halle, (2) Fraunhofer-Institut für Werkstoffmechanik IWM, Halle, and (3) BASF, Ludwigshafen

**Funding:** DFG SFB/TRR 102 (Polymers under multiple constraints)

## 2.11 IR transition moment orientational analysis (IR-TMOA) on the surface-induced orientation in thin layers of a high electron mobility n-type copolymer (P[NDI2OD-T2])

A. M. Anton, R. Steyrlleuthner, W. Kossack, D. Neher, and F. Kremer

The novel IR-based method of infrared transition moment orientational analysis (IR TMOA) is employed to unravel the molecular order in thin layers of the semiconducting polymer *poly[N,N'-bis(2-octyldodecyl)-1,4,5,8-naphthalenediimide-2,6-diy]-alt-5,5'-(2,2'-bithiophene)* (P[NDI2OD-T2]). Structure-specific vibrational bands are analyzed in dependence on polarization and inclination of the sample with respect to the optical axis. By that the molecular order parameter tensor for the respective molecular moieties with regard to the sample coordinate system is deduced. Making use of the specificity of the IR spectral range, we are able to determine separately the orientation of atomistic planes defined through the *naphthalenediimide* (NDI) and *bithiophene* (T2) units relative to the substrate, and hence, relative to each other.

A pronounced solvent effect has been observed: While chlorobenzene causes the T2 planes to align preferentially parallel to the substrate (angle of 29°), 1:1 chloronaphthalene:xylene mixture as solvent results in a *reorientation* of the T2 units from a *face on* arrangement. In contrast the NDI part remains unaffected.[1] The derived orientation is well correlated with the direction of  $\pi$ - $\pi$  stacking.[2] For both solvents evidence for the aggregation of chains in accord with recently published results is obtained by UV/Vis absorption spectroscopy.[1,2]

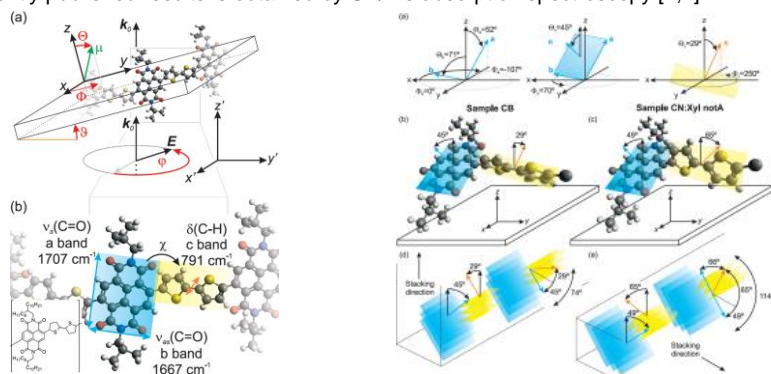


Fig. 1: (a) For IR-TMOA the sample coordinate system ( $x, y, z$ ) is inclined relative to the laboratory frame ( $x', y', z'$ ) while the polarization ( $\rho$ )- and inclination ( $\theta$ )-dependent absorbance is measured. (b) Schematic of a sample fragment and the transition moments (arrows). The  $C_8H_{17}$  and  $C_{10}H_{21}$  alkyl side chains are replaced by methyl groups.

Fig. 2: (a) Microscopic orientation of the molecular planes. (b) Using chlorobenzene, the NDI unit (blue) is inclined by 45° relative to the substrate, whereas the T2 part (yellow) features an angle of 29° and a *face on* orientation. (c) Using a chloronaphthalene:xylene mixture results in a distinct *edge on* orientation of the T2 unit. The NDI block, instead, retains its alignment. For sake of clarity the  $C_8H_{17}$  and  $C_{10}H_{21}$  alkyl chains are replaced by methyl groups. (d,e) Interpretation of the  $\pi$ - $\pi$  stacking direction correlated to the orientation of the T2 unit.

### References:

- [1] A. M. Anton, R. Steyrlleuthner, W. Kossack, D. Neher, F. Kremer, manuscript in preparation  
 [2] R. Steyrlleuthner, R. Di Pietro, et al., D. Neher, J. Am. Chem. Soc. (2014) **136**, 4245-4256

**Collaborations:** (1) Universität Potsdam and (2) Freie Universität Berlin

**Funding:** DFG SFB/TRR 102 (Polymers under multiple constraints)

## 2.4 Structure and Dynamics of Asymmetric Poly(styrene-*b*-1,4-isoprene) Diblock Copolymer under 1D and 2D Nanoconfinement

W. K. Kipnusu, M.M. Elmahdy, E. U. Mapesa, J. Zhang, W. Böhlmann D-M. Smilgies, C. M. Papadakis and F. Kremer

From both technological and fundamental view points, studies of structure and dynamics of confined block copolymers (BCPs) is of great interest. In most technological applications, BCPs are constrained within nano-scale spaces of different dimensions. The question of how dimensionality of nanoconfinement affects the morphologies and the dynamical properties such as glass transition temperature of BCPs therefore become weighty. In this work the impact of 1- and 2-dimensional (2D) confinement on the structure and dynamics of asymmetric poly(styrene-*b*-1,4-isoprene) P(S-*b*-I) with  $f_{PI} = 0.73$  diblock copolymer is investigated by a combination of Scanning Electron Microscopy (SEM), Atomic Force Microscopy (AFM), Grazing-Incidence Small-Angle X-ray Scattering (GISAXS), and Broadband Dielectric Spectroscopy (BDS). 1D confinement is achieved by spin coating the P(S-*b*-I) to form nanometric thin films on silicon substrates, while in the 2D confinement, the copolymer is infiltrated into cylindrical anodized aluminum oxide (AAO) nanopores. Figure 1 shows the SEM and GISAXS results for the sample confined in AAO pores and in thin films respectively. The SEM micrograph reveal copolymer nanorods. GISAXS images of thin films show hexagonally packed cylinders. Three dielectrically active relaxation modes assigned to the two segmental modes of the styrene and isoprene blocks and the normal mode of the latter are studied selectively by BDS. The dynamic glass transition, related to the segmental modes of the styrene and isoprene blocks is independent of the dimensionality and the finite sizes (down to 18 nm) of confinement but the normal mode is influenced by both factors with 2D geometrical constraints exerting greater impact. This reflects the considerable difference in the length scales on which the two kinds of fluctuations take place.[1]

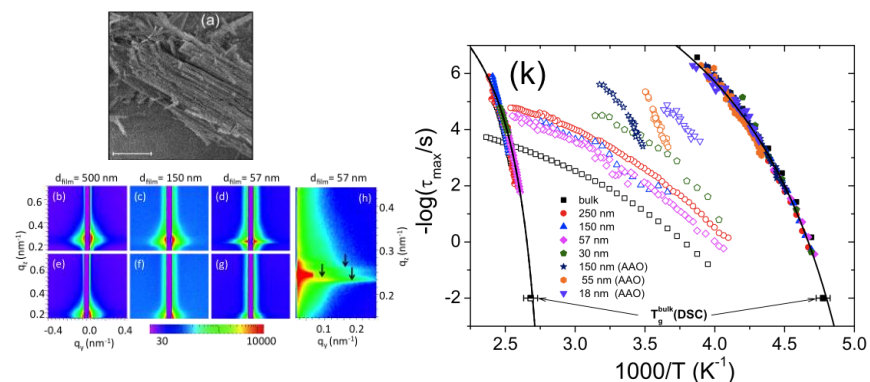


Fig. 1: SEM micrograph of the nanorods of P(S-*b*-I) that was contained in 150 nm AAO pores (a); 2D GISAXS images of P(S-*b*-I) films with  $f_{PI} = 0.73$  (b-d, h)  $\alpha_i = 0.14^\circ$  and (e-g)  $\alpha_i = 0.09^\circ$  and activation plot for the relaxation processes in P(S-*b*-I) (k). The film thicknesses and pore sizes are indicated.

### References:

- [2] W.K. Kipnusu, M.M. Elmahdy, J. Zhang, W. Böhlmann D-M. Smilgies, C. M. Papadakis and F. Kremer, Submitted to ACS Appl. Mater. Interfaces, (2014).

**Funding:** SFB/TRR 102 within the project 'polymers under multiple constraints'

## 2.5 Hydrogen-bonded chain length equilibria in mono-hydroxyl alcohol under nano-confinement.

W.K.Kipnusu, K. Kaminiski, and F. Kremer

The effect of 2-D confinement of 2-ethyl-1-hexanol (2E1H) in unidirectional nano-pores having diameters of 4, 6, and 8 nm as studied by means of Broadband Dielectric (BDS) and Fourier Transform Infrared (FTIR) spectroscopies. The glassy dynamics of confined 2E1H is faster than bulk at the vicinity of  $T_g$  while the Debye relaxation is minimally affected. The decrease in the ratio of dielectric strength of these two processes, and a weakening of the dipolar correlation is accompanied by a concomitant increase in the population of isolated molecules as revealed by FTIR. In hydrophilic pores, the apparent thickness of interfacial layer obtained from BDS decreases with temperature in accord with the FTIR data. This proves that geometrical constraints and the surface interactions break the linear chains in 2E1H resulting in shorter Hydrogen bonded structures that still exhibit Debye-like relaxation. [1]

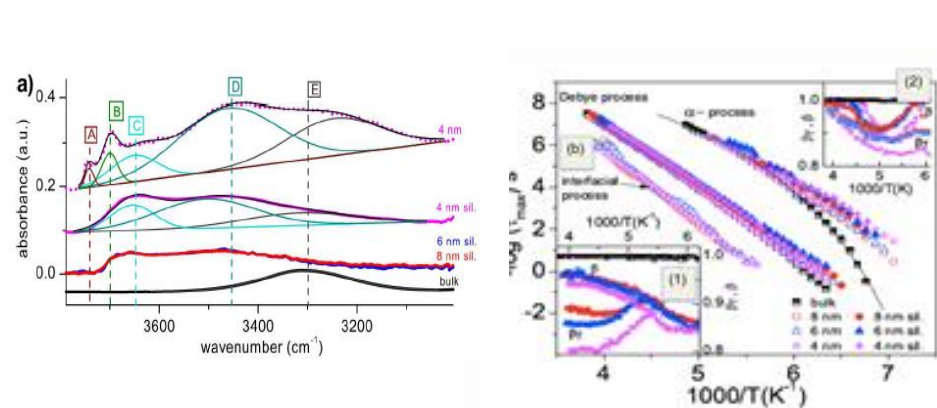


Fig. 1. (a) shows stacked infrared spectra of 2E1H at 255 K (thick lines) in bulk and when confined in different pore sizes being modeled as a sum (black, thin lines) of independent pseudo-voigt peaks (colored thin lines). (a) All absorption peaks are assigned to  $\nu(\text{OH})$  of the various hydroxyl groups present in the system: silica surface (non H-bonded): A; silica surface (H-bond donor): B; isolated 2E1H: C; terminal 2E1H in chains (H-bond donor): D; and bulky 2E1H (H-bond donor and acceptor): E. (b) Activation plots for 2E1H; in bulk state (half-filled symbols), in native silica pores (open symbols) and in silanized pores (filled symbols). Insets: Temperature dependence of the HN shape parameters of the Debye process:  $\beta$  and  $\beta\gamma$  for: (1) silanized and (2) native silica nanopores.

### References:

[1] W.K.Kipnusu, K. Kamil, and F. Kremer *under preparation*

### Funding:

DFG: SFB/TRR 102 within the project 'polymers under multiple constrains'

## 2.10 Methods to determine the pressure dependence of the molecular order parameter in (bio)macromolecular fibers

A. M. Anton, C. Gutsche, W. Kossack, and F. Kremer

The experimental realization and an algorithm for analyzing the pressure dependence of the molecular order parameter of specific structural moieties in (bio)macromolecular fibers has been developed. By employing a diamond anvil cell (DAC) the polarization-dependent IR-transmission at hydrostatic pressure is recorded. In parallel, using an integrated microscope, the macroscopic orientation of the fibers is determined. Because the apparent spectral dichroism originates from the *convolution* of the *macroscopic distribution* of the fibers and the *microscopic distribution* of transition moments within one fiber, one is able to separate between order and disorder at macroscopic and microscopic scales. Using the example of major ampullate spider silk the pressure dependence of the molecular order parameter of alanine groups located within nanocrystalline building blocks is deduced and found to decrease reversibly by 0.01 GPa<sup>-1</sup> when varying the external hydrostatic pressure between 0 and 3 GPa.

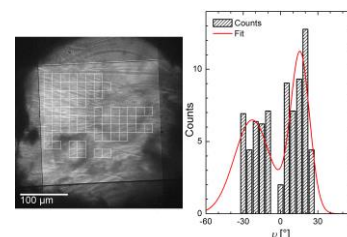


Fig. 1: The macroscopic orientation distribution of the fibers is evaluated by determining the mean orientation within a reference volume (square region) and compiling a histogram or distribution function of these reference volumina.

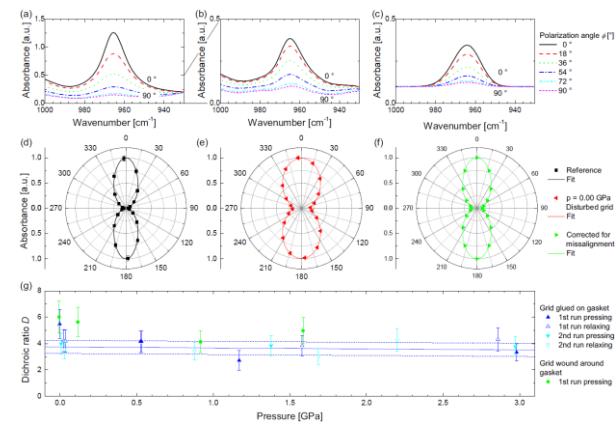


Fig. 2: (a) The spectral dichroism of parallel fibers is used as a standard for the microscopic distribution of transition moments at ambient conditions (d). (b) Applying hydrostatic pressure causes the grating of parallel fibers to distort on expense of the apparent dichroism (e). (c) Utilizing the macroscopic distribution of the fibers (Fig. 1) and anticipate the apparent dichroism as the convolution of the macroscopic distribution and the microscopic distribution of the transition moments within one fiber one is able to separate pressure effects on the macroscopic and microscopic scale and to extract the microscopic transition moment distribution for a deformed grating. (g) This procedure is used to determine the pressure dependence of the molecular order parameter of an alanine-specific vibration located within the nanocrystallites.[1]

### References:

[1] A. M. Anton, C. Gutsche, W. Kossack, F. Kremer, *Soft Matter* (2014) DOI: 10.1039/C4SM01142B

### Collaborations:

Funding: (1) DFG SFB/TRR 102 (Polymers under multiple constraints) and (2) BuildMoNa

## 2.9 Glassy dynamics of Poly(2-Vinyl-Pyridine) brushes with varying grafting density

N. Neubauer, R. Winkler, M. Treß, P. Uhlmann, M. Reiche and F. Kremer

The molecular dynamics of poly(2-vinyl-pyridine) (P2VP) brushes is measured by Broadband Dielectric Spectroscopy (BDS) in a wide temperature (250K – 440K) and broad spectral (0.1 Hz – 1 MHz) range. This is realized using a nanostructured electrode arrangement. Two highly conductive silicon electrodes ( $\rho < 0.01 \Omega\text{cm}$ ) are assembled to form the capacitor. Silicon dioxide pistons having a height of 35 nm serve as spacers, leading to a distance of around 40 - 50 nm between the solid surfaces of the electrodes. The grafting of P2VP on a highly conductive silicon layer is realized in a two-step “grafting-to” preparation. A thin layer ( $\approx 2.5$  nm) of poly(glycidyl methacrylate) (PGMA) serves as anchors for carboxyl terminated poly(2-vinylpyridine) (P2VP-COOH). By applying different annealing times, P2VP-brushes with different grafting densities are formed. In the present study P2VP-brushes with five grafting densities (0.03 – 0.117 chains/nm<sup>2</sup>) and layer thicknesses from 2 nm to 7 nm were investigated. This corresponds to distances between the grafting points of about 3 - 6 nm (smaller than  $2R_g \approx 10$  nm). The quality of the prepared films is checked by ellipsometry and Atomic Force Microscopy (AFM). The dielectric loss  $\epsilon''$  spectra show two well separated relaxation modes, an Arrhenius-like process being attributed to fluctuations in the poly(glycidyl methacrylate) (PGMA) linker used for the grafting reaction and the segmental dynamics (dynamic glass transition) of the P2VP brushes (Fig.1 a). The latter is characterized by a Vogel-Fulcher-Tammann dependence similar to bulk P2VP (Fig. 1 b). The results can be comprehended considering the length scale on which the dynamic glass transition ( $\leq 1$  nm) takes place.

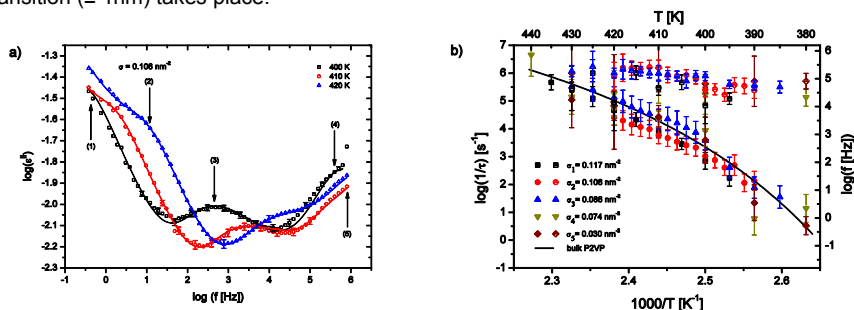


Fig. 1: a) Dielectric loss  $\epsilon''$  spectra of P2VP brushes with  $\sigma = 0.106 \text{ nm}^{-2}$  on a PGMA anchoring layer at varying temperatures as indicated. Several contributions are observed and marked by arrows in the spectra. (1) a linear contribution due to a parasitic conductivity of the spacers or contaminating particles between the electrodes, (2) a polarization which originates from the conductivity of P2VP, (3) the  $\alpha$ -relaxation of P2VP, (4) a PGMA-relaxation, (5) and a linear contribution due to the limited conductivity of the silicon electrodes. The fit function (solid lines) is deduced from an equivalent circuit model.

b) Activation plot of the P2VP  $\alpha$ -relaxation (filled symbols) and the PGMA-relaxation (half-filled symbols) for five different grafting densities as indicated. For all grafting densities the PGMA relaxation has an Arrhenius-like thermal activation while the P2VP-brushes follow a Vogel-Fulcher-Tammann temperature dependence. The solid line shows the mean relaxation rates of bulk P2VP. The error bars show the accuracy for determining the mean relaxation rate.

### Collaborations:

- [1] Leibniz Institute of Polymer Research, Dresden
- [2] Max-Planck-Institute of Microstructure Physics, Halle
- [3] MicroFAB, Bremen

## 2.6 Inter- and intra-molecular dynamics in polyalcohols during glass transition

L. Popp, W. Kossack, M. Treß, W.K. Kipnusu and F. Kremer

The molecular dynamics of a homologous series of glass forming polyalcohols is studied by Broadband dielectric spectroscopy (BDS) and Fourier transform infrared spectroscopy (FTIR) during the dynamic glass transition around the calorimetric glass transition temperature,  $T_g$  [1]. Using BDS, the dynamics of dielectric relaxation processes are investigated in sorbitol, xylitol, threitol and glycerol over a wide frequency range ( $10^{-2}$  to  $10^6$  Hz). Additionally, FTIR is utilized to characterize the temperature dependence of *intra*-molecular vibrations of different atom bonds [2]. Therefore, the temperature dependencies of specific IR absorption bands are studied in terms of their spectral position and the corresponding oscillator strength. By comparison of the results from BDS and FTIR the different properties and the interplay between *inter*- and *intra*-molecular dynamics can be examined [3].

With decreasing temperature the IR band positions of the CCO and CO stretching vibration and the  $\text{CH}_2$  twisting vibration, show a blue shift with a distinct kink at the calorimetric glass transition temperature. The OH stretching vibration again exhibits a different temperature dependency, namely a strong redshift with decreasing temperature. Additionally, a qualitative model of the underlying molecular causes to the obtained vibrational dynamics is developed.

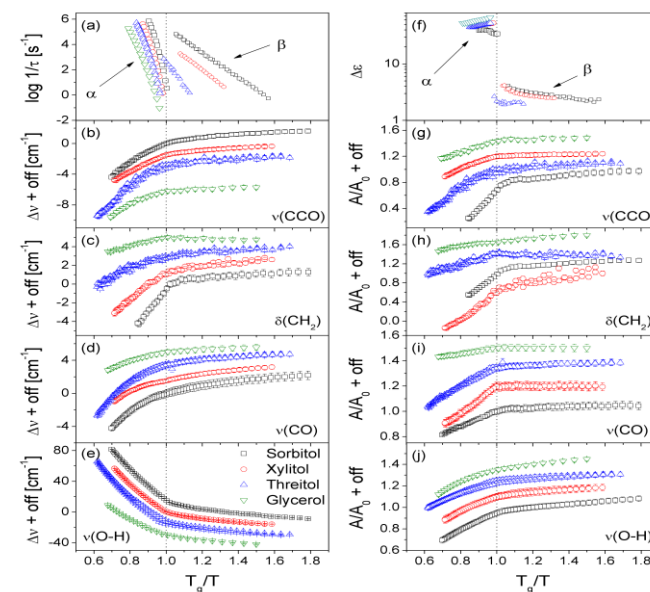


Fig. 1: Comparison of the IR vibrational properties (from FTIR) and the relaxation dynamics (from BDS) of sorbitol, xylitol, threitol and glycerol as a function of scaled T (with respective  $T_g$ ). The (a) activation plots and (f) the relaxation strengths (from BDS) of the  $\alpha$ - and  $\beta$ -relaxations are shown as well as the temperature dependencies of the peak positions (b-e) of the different investigated *intra*-molecular vibrations and their corresponding oscillator strengths (g-j) (with arbitrary offsets between curves).

### References:

- [1] P. Papadopoulos et al., Soft Matter (2013) **9**, 1600-1603
- [2] W. Kossack et al., Phys Chem Chem Phys (2013), **15**(47): 20641-50
- [3] W. K. Kipnusu et al., Soft Matter (2013) **9**, 4681-4686.

## 2.7 Relaxations and charge transport in Polymeric Ionic Liquids

F. Frenzel, M. Y. Folikumah<sup>1</sup>, M. Schulz<sup>1</sup>, W. H. Binder<sup>1</sup>, F. Kremer

<sup>1</sup> Institute of Chemistry, Martin-Luther-University Halle-Wittenberg, Von-Danckelmann-Platz4, 06120 Halle, Germany

Broadband Dielectric Spectroscopy (frequency range:  $10^{-2}$ - $10^7$ Hz, temperature range: 200-400K) as well as calorimetry are employed to unravel relaxations and charge transport in a homologous series of monovalent or bivalent N,N,N-triethyl-ammonium and 1-methylpyrrolidinium telechelic polyiso-butylene (PIB) based Polymeric Ionic Liquids (PIL) (Fig.1) having four different anions (Br, NTf<sub>2</sub>, OTf, pTOS).

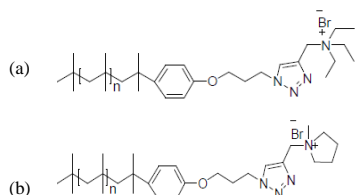


Fig. 1: Chemical structure of N,N,N-triethylammonium telechelic PIB (a) and of 1-methylpyrrolidinium telechelic PIB (b) (here with bromide as anion).

Two relaxation processes are observed, being assigned to the dynamic glass transitions of the polymeric part of the PIL and to the moieties having the character of Ionic liquids. The former (Fig.2) scales well with the calorimetric glass transition temperature as measured calorimetrically; the latter (Fig.3) is proportional in its relaxation rate to the DC conductivity, hence following a Barton-Nakajima-Namikawa (BNN) relation as well established for low molecular weight systems.

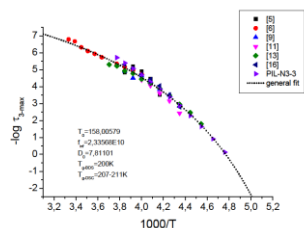


Fig. 2: Five samples, where the dynamic glass transition relaxation can be observed, as well as the polymeric part of the PIL and a general Vogel-Fulcher-Tamman-fit.

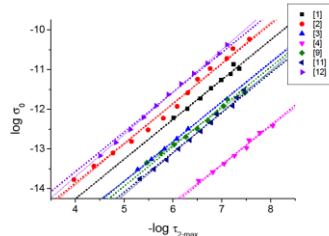


Fig. 3: Seven selected samples that show strongly the linear dependency between relaxation time of the second process and the dc-conductivity, whereat the straight lines reveal a linear fit resp. to the data and the dotted line resp. to slope value 1.

### References:

- [1] Sangoro, J.R., C. Iacob, A.L. Agapov, Y. Wang, S. Berdzinski, H. Rexhausen, V. Strehmel, C. Friedrich, A.P. Sokolov, F. Kremer, "Decoupling of ionic conductivity from structural dynamics in polymerized ionic liquids" *Soft Matter* **10**, (20) 3536-402014 (2014) DOI: 10.1039/c3sm53202j[2]
- [2] Sangoro, J.R., F. Kremer, "Charge transport and glassy dynamics in ionic liquids" *Acc. Chem. Res.* **45** (4), 525-532 (2012) DOI: 10.1021/ar2001809
- [3] Sangoro, J.R., M. Mierzwa, C. Iacob, M. Paluch, F. Kremer, "Brownian dynamics determine the universality of charge transport in ionic liquids" *RSC Adv.* **2**, 5047-5050 (2012) DOI: 10.1039/C2RA20560B

**Funding:** DFG: - KR-1138/24-1 / STR-437/7-1

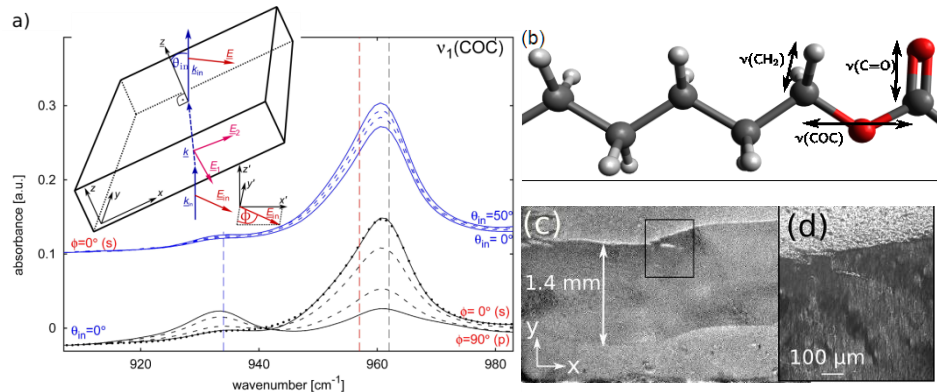
**Collaboration:** Prof. Dr. Strehmel, Hochschule Niederrhein, Institute of Organic Chemistry, 47798 Krefeld, Germany

## 2.8 Strain induced, anisotropic crystallization studied by FTIR

W. Kossack, A. Seidlitz\*, T. Thurn-Albrecht\*, F. Kremer

\*Institut für Physik, Martin-Luther-Universität Halle-Wittenberg, von-Danckelman-Platz 3, 06120 Halle, Germany

The orientation of crystalline and amorphous building blocks in strain-recrystallized Poly-Caprolactone (PCL, Fig. b) is studied by Infrared-Transition Moment Orientational Analysis (Fig. a shows the corresponding IR-spectra) [1]. To do so a cast film is stretched by approximately 10% leading to a plastically deformed region (PDR,  $\sim 2\mu\text{m}$  thick) and an elastically deformed region (EDR,  $\sim 8\mu\text{m}$ ). As apparent from Polarized optical microscopy (POM) both regions exhibit anisotropic optical properties on the length-scale of the wavelength (Fig. c,d). In the PDR the initially centrosymmetrically grown spherulites are broken up and linear structures are formed (Fig. d), exhibiting a strong macroscopic ( $\sim \text{cm}^2$ ) and biaxial order of crystalline and amorphous moieties. This is quantified by the nematic order parameter  $S$ , being  $\leq 0.76$  for the crystalline  $c$ -axes and  $\leq 0.5$  for the amorphous chains' backbones. The respective biaxiality,  $b$ , is found to be  $\sim 0.25$  and  $\sim 0.1$  [1]. This is in contrast to the EDR, where  $S \sim b \sim 0$ .



a) IR-spectra of the PDR measured for different polarizations  $\Phi$  and inclinations  $\theta_{in}$  as given in the graph; The inset shows the geometry of the measurement including the electric fields,  $\vec{E}$  and the wavevectors,  $\vec{k}$ . b) IR spectra b) chemical structure (stick and ball model) and transition moments (arrows) of the PCL monomer (light grey: H, dark grey C and red O); c) micrograph of the PDR; The framed region is depicted in d) showing a POM picture.

### References:

- [1] W. Kossack, P. Papadopoulos, P. Heinze, H. Finkelman and F. Kremer, *Macromolecules*, vol. 43, no. 18, 7532-7539, 2010.

**Funding:** BuildMoNa, FOR 877, SFB-TRR 102